

Fluid analog model for boundary effects in field theory

L. H. Ford*

Institute of Cosmology, Department of Physics and Astronomy, Tufts University, Medford, Massachusetts 02155, USA

N. F. Svaiter†

Centro Brasileiro de Pesquisas Físicas-CBPF, Rua Dr. Xavier Sigaud 150, Rio de Janeiro, RJ, 22290-180, Brazil
(Received 16 March 2009; revised manuscript received 8 September 2009; published 30 September 2009)

Quantum fluctuations in the density of a fluid with a linear phonon dispersion relation are studied. In particular, we treat the changes in these fluctuations due to nonclassical states of phonons and to the presence of boundaries. These effects are analogous to similar effects in relativistic quantum field theory, and we argue that the case of the fluid is a useful analog model for effects in field theory. We further argue that the changes in the mean squared density are, in principle, observable by light scattering experiments.

DOI: 10.1103/PhysRevD.80.065034

PACS numbers: 42.50.Lc, 03.70.+k, 05.40.-a

I. INTRODUCTION

It is well known that quantized sound waves, whose excitations are phonons, share several properties with relativistic quantum fields, such as the electromagnetic field. This is especially true when the phonon dispersion relation is approximately linear, which will be assumed throughout this paper. There is a phononic analog of the usual Casimir effect, but it tends to be quite small. For example, the force on two parallel plates due to phonon zero-point energy is smaller than that in the electromagnetic case by the ratio of the speed of sound in the fluid to the speed of light [1]. This ratio is typically of order 10^{-6} . However, forces due to classical stochastic sound fluctuations have been discussed recently by several authors [2–7], and can be larger. Here we will study the local changes in density fluctuations of a fluid due either to the presence of boundaries or to changes in the quantum state of the phonons. This is an analog of the effect of boundaries on the quadratic expectation values of relativistic quantum fields, such as the mean squared electric field. In a related context, Unruh [8] has shown that the velocity potential ϕ , of a moving fluid with velocity $\mathbf{v} = \nabla\phi$, satisfies the same equation as does a relativistic scalar field in a curved spacetime. The present paper is an expanded version of Ref. [9]. We begin in Sec. II by reviewing the quantization of sound waves in a fluid and the calculation of the density correlation function. We review recent work on the scattering of light by zero-point fluctuations in a fluid in Sec. III A, and then discuss thermal corrections in Sec. III B. In Sec. IV, we consider the effects of a squeezed state of phonons on the local density fluctuations. The effects of boundaries are treated in Sec. V, where several different geometries are discussed. The operational meaning of these results is discussed in Sec. VI, where we give estimates for the effects of boundaries on

the light scattering cross section. Our results are summarized and discussed in Sec. VII.

II. QUANTIZATION AND THE DENSITY CORRELATION FUNCTION

We consider the quantization of sound waves in a fluid with a linear dispersion relation, $\Omega_q = c_S q$, where Ω_q is the phonon angular frequency, q is the magnitude of the wave vector, and c_S is the speed of sound in the fluid. This should be a good approximation for wavelengths much longer than the interatomic separation. Let ρ_0 be the mean mass density of the fluid. Then the variation in density around this mean value is represented by a quantum operator, $\hat{\rho}(\mathbf{x}, t)$, which may be expanded in terms of phonon annihilation and creation operators as [10]

$$\hat{\rho}(\mathbf{x}, t) = \sum_{\mathbf{q}} (b_{\mathbf{q}} f_{\mathbf{q}} + b_{\mathbf{q}}^{\dagger} f_{\mathbf{q}}^*), \quad (1)$$

where

$$f_{\mathbf{q}} = \sqrt{\frac{\hbar\omega\rho_0}{2Vc_S^2}} e^{i(\mathbf{q}\cdot\mathbf{x} - \Omega_q t)}. \quad (2)$$

Here V is a quantization volume. The normalization factor in Eq. (2) can be fixed by requiring that the zero-point energy of each mode be $\frac{1}{2}\hbar\Omega_q$ and using the expression for the energy density in a sound wave,

$$U = \frac{c_S^2}{\rho_0} \hat{\rho}^2. \quad (3)$$

In the limit in which $V \rightarrow \infty$, we may write the vacuum density correlation function as

$$\langle \hat{\rho}(\mathbf{x}, t) \hat{\rho}(\mathbf{x}', t') \rangle_0 = \frac{\hbar\rho_0}{16\pi^3 c_S^2} \int d^3q \Omega_q e^{i(\mathbf{q}\cdot\Delta\mathbf{x} - \Omega_q \Delta t)}, \quad (4)$$

where $\Delta\mathbf{x} = \mathbf{x} - \mathbf{x}'$ and $\Delta t = t - t'$. The integral may be evaluated to write the coordinate space correlation function as

*ford@cosmos.phy.tufts.edu
†nfluxvai@cbpf.br

$$\langle \hat{\rho}(\mathbf{x}, t) \hat{\rho}(\mathbf{x}', t') \rangle_0 = -\frac{\hbar \rho_0}{2\pi^2 c_S} \frac{\Delta \mathbf{x}^2 + 3c_S^2 \Delta t^2}{(\Delta \mathbf{x}^2 - 3c_S^2 \Delta t^2)^3}. \quad (5)$$

This is of the same form as the correlation function for the time derivative of a massless scalar field in relativistic quantum field theory, $\langle \dot{\phi}(\mathbf{x}, t) \dot{\phi}(\mathbf{x}', t') \rangle$. (This analogy has been noted previously in the literature. See, for example, Ref. [11].) Apart from a factor of ρ_0 , these two quantities may be obtained from one another by interchanging the speed of light c and the speed of sound c_S . If $c \rightarrow c_S$ and a factor of ρ_0 is added, then

$$\langle \dot{\phi}(\mathbf{x}, t) \dot{\phi}(\mathbf{x}', t') \rangle \rightarrow \langle \hat{\rho}(\mathbf{x}, t) \hat{\rho}(\mathbf{x}', t') \rangle_0. \quad (6)$$

Note that we are using a convention for the scalar field in which $(\nabla \phi)^2$ has dimensions of energy density, so $\dot{\phi}^2$ has dimensions of mass density.

In the limit of equal times, the density correlation function becomes

$$\langle \hat{\rho}(\mathbf{x}, t) \hat{\rho}(\mathbf{x}', t) \rangle_0 = -\frac{\hbar \rho_0}{2\pi^2 c_S (\Delta \mathbf{x})^4}. \quad (7)$$

Thus the density fluctuations increase as $|\Delta \mathbf{x}|$ decreases. Of course, the continuum description of the fluid and the linear dispersion relation both fail as $|\Delta \mathbf{x}|$ approaches the interatomic separation. Also note the minus sign in Eq. (7). This implies that density fluctuations at different locations at equal times are anticorrelated. By contrast, when $c_S |\Delta t| > |\Delta \mathbf{x}|$, then $\langle \hat{\rho}(\mathbf{x}, t) \hat{\rho}(\mathbf{x}', t) \rangle > 0$ and the fluctuations are positively correlated. This is in complete analogy with the situation in the relativistic theory. Fluctuations inside the light cone can propagate causally and tend to be positively correlated. Fluctuations in a fluid for which $c_S |\Delta t| < |\Delta \mathbf{x}|$ cannot have propagated from one point to the other, and are anticorrelated. This can be understood physically because an overdensity of fluid at one point in space requires an underdensity at a nearby point.

III. LIGHT SCATTERING BY DENSITY FLUCTUATIONS

A. Scattering by zero-point fluctuations

In Ref. [12], the cross section for the scattering of light by the zero-point density fluctuations is computed for the case that the incident light angular frequency is large compared to the typical phonon frequency. The result is

$$\left(\frac{d\sigma}{d\Omega} \right)_{ZP} = \sqrt{2(1 - \cos\theta)} \frac{\hbar \omega^5 \mathcal{V} \eta^4}{32\pi^2 c_S^5 \rho_0} (\hat{\mathbf{e}}_{\mathbf{k}, \lambda} \cdot \hat{\mathbf{e}}_{\mathbf{k}', \lambda'})^2, \quad (8)$$

where θ is the scattering angle, \mathcal{V} is the scattering volume, and η is the mean index of refraction of the fluid. In addition, $\hat{\mathbf{e}}_{\mathbf{k}, \lambda}$ and $\hat{\mathbf{e}}_{\mathbf{k}', \lambda'}$ are the initial and final polarization vectors, respectively. The ω^5 dependence of the scattering cross section can be viewed as the product of the ω^4 dependence of Rayleigh-Brillouin scattering and one power of ω coming from the spectrum of zero-point fluctuations

in the fluid. The factor of η^4 represents the influence of the fluid on light propagation before and after the scattering process, and arises as a product of a factor of η in the incident flux and a factor of η^3 in the density of final states [12]. Because light travels through the fluid at speeds much greater than the sound speed, light scattering reveals a nearly static distribution of density fluctuations. Thus we can regard Eq. (8) as a probe of the fluctuations described by Eq. (7). The scattering by zero-point fluctuations is inelastic, with the creation of a phonon. Thus, the scattering described by Eq. (8) is strictly Brillouin rather than Rayleigh scattering.

This scattering by zero-point density fluctuations should be compared to the effects of thermal density fluctuations. The ratio of the zero point to the thermal scattering for the Stokes line may be expressed as

$$R \equiv \frac{(d\sigma/d\Omega)_{ZP}}{(d\sigma/d\Omega)_{TB}} = \sqrt{2(1 - \cos\theta)} \left(\frac{\hbar \omega}{2k_B T} \right) \left(\frac{c_S}{c} \right) \eta^4 \left[\rho_0 \left(\frac{\partial \epsilon}{\partial \rho_0} \right)_S \right]^{-2}. \quad (9)$$

The index of refraction, η , and the quantity $\rho_0 (\partial \epsilon / \partial \rho_0)_S$, which involves a derivative of the fluid dielectric function with respect to density at constant entropy, are both of order unity. Hence R is primarily determined by the ratio of the photon energy to the thermal energy, and the ratio of the speed of sound to the speed of light.

B. Finite temperature effects

Note that the zero-point scattering cross section, Eq. (8), is the sole cross section at zero temperature. At finite temperature, the Stokes line cross section (describing the process in which a phonon is emitted) is modified by the factor

$$\langle n_{\mathbf{q}} \rangle + 1 = \frac{1}{e^{\hbar \Omega_{\mathbf{q}} / kT} - 1} + 1, \quad (10)$$

where $\langle n_{\mathbf{q}} \rangle$ is the mean number of phonons in mode \mathbf{q} and $\hbar \Omega_{\mathbf{q}}$ is the phonon energy. In the low temperature limit, $kT \ll \hbar \Omega_{\mathbf{q}}$, this correction factor goes to unity, giving the zero-point result. In the high temperature limit, $kT \gg \hbar \Omega_{\mathbf{q}}$, it becomes

$$\langle n_{\mathbf{q}} \rangle + 1 \sim \frac{kT}{\hbar \Omega_{\mathbf{q}}} + \frac{1}{2} + O(1/T). \quad (11)$$

The leading term is the usual high temperature limit. The next term is the zero-point effect, giving rise to a contribution to the cross section proportional to ω^5 . More precisely, it is 1/2 of the zero-point effect, the other 1/2 having been canceled by the thermal correction. Our view is that zero-point fluctuations are always present at all temperatures, but in this case the thermal correction partially masks the zero-point effect. However, the half which remains is potentially observable. For experiments

in the high temperature limit, the ω^5 part of the cross section is given by 1/2 of the right-hand side of Eq. (8).

Some numerical estimates for various fluids are given in Ref. [12] for violet light with a wavelength of $\lambda = 350$ nm. For the case of liquid neon, $R \approx 0.13$, so that about 13% of the Stokes line is due to zero-point motion effects [13], which might be detectable experimentally. Even in the case of water at room temperature, $R \approx 0.004$. Although small in absolute terms, this is surprisingly large for a macroscopic quantum effect at room temperature.

It is interesting to note that if one were to look only at the total Brillouin cross section (Stokes plus anti-Stokes), the zero-point effect would be masked at high temperatures. The anti-Stokes line describes phonon absorption, so in the limit that $\omega \gg \Omega_q$, its cross section is of the same form as that for the Stokes line, but its thermal correction factor is $\langle n_q \rangle$. The total cross section from both lines has a factor of

$$2\langle n_q \rangle + 1 = \coth\left(\frac{\hbar\Omega_q}{2kT}\right) \sim \frac{2kT}{\hbar\Omega_q} + O(1/T),$$

$$kT \gg \hbar\Omega_q. \quad (12)$$

Here the thermal part completely masks the zero-point part, leaving a residue of order $1/T$. The same masking effect also occurs for the energy of a collection of harmonic oscillators, which is proportional to the quantity in Eq. (12). The thermal effect on scattering is often described by a structure factor. See, for example, Ref [14]. The hyperbolic cotangent form of the structure factor, corresponding to Eq. (12), was calculated in Ref. [15].

The key result of this subsection is that zero-point effects can be distinguished from thermal effects, even at relatively high temperature. If one examines only the Stokes line, for which Eq. (11) applies, then the ratio of the thermal part to the zero-point part is the ratio R . Even when this ratio is small in magnitude, the linear temperature dependence of the thermal terms can allow these two effects to be distinguished.

IV. SQUEEZED STATES OF PHONONS

Here we consider the case where the phonon field is not in the vacuum state, but rather a squeezed state. Thus in this section, we will be concerned with state-dependence effects as opposed to boundary effects. However, the two effects are closely analogous.

The squeezed states are a two-complex-parameter family of states in which the quantum uncertainty in one variable can be reduced with a corresponding increase in the uncertainty of the conjugate variable. See, for example, Refs. [16,17] for a detailed treatment of the properties of the squeezed states. We will focus our attention on the case of the squeezed vacuum states $|\zeta\rangle$ for a single mode, labeled by a single complex squeeze parameter

$$\zeta = re^{i\delta}, \quad (13)$$

and defined by

$$|\zeta\rangle = S(\zeta)|0\rangle. \quad (14)$$

Here

$$S(\zeta) = e^{(1/2)[\zeta^* a^2 - \zeta(a^\dagger)^2]} \quad (15)$$

is the squeeze operator and a and a^\dagger are phonon annihilation and creation operators for the selected mode. This set of states is of special interest because they are the states generated by quantum particle creation processes, and they can exhibit local negative energy densities. (See, for example, Refs. [18,19].)

Consider the shift in the mean squared density fluctuations between the given state and the vacuum,

$$\langle \hat{\rho}^2 \rangle_R = \langle \zeta | \hat{\rho}^2 | \zeta \rangle - \langle 0 | \hat{\rho}^2 | 0 \rangle, \quad (16)$$

the ‘‘renormalized’’ mean squared density fluctuation. The result for this quantity in a single mode squeezed vacuum state for a plane wave in the z direction is

$$\langle \hat{\rho}^2 \rangle_R = \frac{\hbar\omega\rho_0}{c_S^2 V} \sinh r \{ \sinh r - \cosh r \cos[2(kz - \omega t) + \delta] \}. \quad (17)$$

Here we have used the identities

$$S^\dagger(\zeta)aS(\zeta) = a \cosh r - a^\dagger e^{i\delta} \sinh r \quad (18)$$

and

$$S^\dagger(\zeta)a^\dagger S(\zeta) = a^\dagger \cosh r - a e^{-i\delta} \sinh r. \quad (19)$$

Note that the quantity in Eq. (17) can be either positive or negative, but its time or space average is positive. The suppression of the local density fluctuations in a squeezed state is analogous to the creation of negative energy densities for a massless, relativistic field. [Compare Eq. (17) with Eq. (48) and Fig. 8 in Ref. [19].]

Thus the creation of a squeezed state of phonons can suppress the local density fluctuations just as a squeezed state of photons can produce local negative energy density.

V. BOUNDARIES

If we introduce an impenetrable boundary into the fluid, the phonon field will satisfy Neumann boundary conditions

$$\hat{\mathbf{n}} \cdot \nabla \delta\rho = 0 \quad (20)$$

as a consequence of the impenetrability. Thus there will be a Casimir force on the boundaries which is analogous to the Casimir force produced by electromagnetic vacuum effects. For example, consider two parallel plates, which will experience an attractive force per unit area of

$$\frac{F}{A} = \frac{\hbar c_S \pi^2}{480 a^4}, \quad (21)$$

which is smaller than the electromagnetic case for perfect

plates by a factor of $c_S/(2c)$, and is thus quite small in any realistic situation.

Henceforth, we consider the local effect of boundaries on mean squared density fluctuations, and now define $\langle \hat{\rho}^2 \rangle_R$ to be the change due to the presence of the boundary. This quantity is of interest both as an analog model for the effects of boundaries in quantum field theory, and in its own right. The shifts in density fluctuations are, at least in principle, observable in light scattering experiments.

Our interest in the phononic analog model is inspired by the fact that the study of boundary effects in quantum field theory is an active area of research, and has given rise to some recent controversies in the literature [20,21]. One question is the nature of the physical cutoff which prevents singularities at the boundary. An example of the subtleties is afforded by the mean squared electric and magnetic fields near a dielectric interface. When the material is a perfect conductor, these quantities are proportional to z^{-4} , where z is the distance to the interface. Specifically, in Lorentz-Heaviside units their asymptotic forms are

$$\langle E^2 \rangle \sim \frac{3\hbar c}{16\pi^2} \frac{1}{z^4} \quad (22)$$

and

$$\langle B^2 \rangle \sim -\frac{3\hbar c}{16\pi^2} \frac{1}{z^4}. \quad (23)$$

One might expect that a realistic frequency-dependent dielectric function would remove this singularity, but this is not the case. Instead one finds [22] that

$$\langle E^2 \rangle \sim \frac{\sqrt{2}\hbar\omega_p}{32\pi} \frac{1}{z^3} \quad (24)$$

and

$$\langle B^2 \rangle \sim -\frac{5\hbar\omega_p^2}{96\pi c} \frac{1}{z^2}, \quad (25)$$

where ω_p is the plasma frequency of the material. Thus some physical cutoff other than dispersion is required. For realistic materials, it is likely to be surface roughness, but fluctuations in the position of the boundary can also serve as a cutoff [23]. In a fluid, there is always a physical cutoff at the interatomic separation.

In the remainder of this paper, we will analyze $\langle \hat{\rho}^2 \rangle_R$ in different geometries. We may write the phonon vacuum density correlation function in the presence of a boundary as

$$G(\mathbf{x}, \mathbf{x}', \Delta t) = G_0(\mathbf{x}, \mathbf{x}', \Delta t) + G_R(\mathbf{x}, \mathbf{x}', \Delta t) \quad (26)$$

where

$$G_0(\mathbf{x}, \mathbf{x}', \Delta t) = \langle \hat{\rho}(\mathbf{x}, t) \hat{\rho}(\mathbf{x}', t') \rangle_0 \quad (27)$$

is the vacuum correlation function in the absence of a boundary, which is given by Eq. (5), and $G_R(\mathbf{x}, \mathbf{x}', \Delta t)$ is the shift in this correlation function due to the presence of a

boundary. Here we treat only the case of static boundaries, so all correlation functions depend on time only through $\Delta t = t - t'$. The shift in mean squared density due to the boundary is then given by the coincidence limit of G_R as

$$\langle \hat{\rho}^2(\mathbf{x}) \rangle_R = G_R(\mathbf{x}, \mathbf{x}', \Delta t)|_{\mathbf{x}=\mathbf{x}', \Delta t=0}. \quad (28)$$

A. One or two parallel plane boundaries

In both of these case, the renormalized density two-point function may be constructed by the method of images. First consider the case of a single plate located at $z = 0$. Let G_0 denote the density correlation function in the absence of a boundary. The two-point function which satisfies the boundary condition Eq. (20) on this boundary is

$$G = G_0(\Delta \mathbf{x}_T, z - z', \Delta t) + G_0(\Delta \mathbf{x}_T, z + z', \Delta t) \quad (29)$$

where \mathbf{x}_T is in the direction transverse to the plate. The renormalized two-point function is

$$G_R = G_0(\Delta \mathbf{x}_T, z + z', \Delta t). \quad (30)$$

The resulting shift in the mean squared density is

$$\langle \hat{\rho}^2 \rangle_R = G_R|_{\mathbf{x}=\mathbf{x}', \Delta t=0} = -\frac{\hbar\rho_0}{32\pi^2 c_S z^4} < 0, \quad (31)$$

where z is the distance to the boundary. For the case of two parallel planes, the correlation function is given by an infinite image sum:

$$G = \sum_{n=-\infty}^{\infty} [G_0(\Delta \mathbf{x}_T, z - z' - 2Ln, \Delta t) + G_0(\Delta \mathbf{x}_T, z + z' - 2Ln, \Delta t)], \quad (32)$$

where L is the plate separation. If we use the identity

$$\begin{aligned} \sum_{n=-\infty}^{\infty} \frac{1}{(n-x)^4} &= \frac{1}{6} \frac{d^2}{dx^2} \sum_{n=-\infty}^{\infty} \frac{1}{(n-x)^2} \\ &= \frac{\pi^2}{6} \frac{d^2}{dx^2} \sum_{n=-\infty}^{\infty} \csc^2(\pi x), \end{aligned} \quad (33)$$

we can obtain the result

$$\langle \hat{\rho}^2 \rangle_R = -\frac{\hbar\rho_0}{96c_S L^4} \left[\frac{1}{15} + \frac{3 - 2\sin^2(\pi z/L)}{\sin^4(\pi z/L)} \right], \quad (34)$$

where z is the distance to one boundary. Note that $\langle \hat{\rho}^2 \rangle_R$ for both of these cases is negative everywhere. In the absence of a physical cutoff, both of these expressions diverge as z^{-4} near the boundaries, just as the squared electric and magnetic fields do near a perfectly reflecting plane. In contrast to the force between two plates, Eq. (21), the shift in mean squared density is inversely proportional to the speed of sound, $\langle \hat{\rho}^2 \rangle_R \propto 1/c_S$. This is a general feature of all shifts in $\langle \hat{\rho}^2 \rangle$ due to boundaries.

B. A three-dimensional torus

Here we consider a rectangular box with periodic boundary conditions in all three spatial directions, with periodicity lengths L_1 , L_2 , and L_3 . Thus the three-dimensional space has the topology of $S^1 \times S^1 \times S^1$. This is closely related to the geometry of a waveguide, where the fluctuations of a relativistic scalar field were discussed by Rodrigues and Svaiter [24]. As in the parallel plane case, an image sum method may be employed to write

$$G = \sum_{\ell, m, n=-\infty}^{\infty} G_0(x - x' + \ell L_1, y - y' + m L_2, z - z' + n L_3, \Delta t). \quad (35)$$

This leads to the result

$$\langle \hat{\rho}^2 \rangle_R = -\frac{\hbar \rho_0}{2\pi^2 c_S} \sum'_{\ell, m, n} \frac{1}{(\ell^2 L_1^2 + m^2 L_2^2 + n^2 L_3^2)^2}. \quad (36)$$

Here the prime on the summation indices denotes that the $\ell = m = n = 0$ term is omitted. In this case, $\langle \hat{\rho}^2 \rangle_R$ is a negative constant.

C. A wedge

Consider two intersecting planes which are at an angle of α with respect to each other. Now consider a point inside of this wedge which is located at polar coordinates (r, θ) , where r is the distance to the intersection line and $\theta < \alpha$. This geometry was treated for the relativistic case by Candelas and Deutsch [25], whose Eq. (5.39) yields

$$\begin{aligned} \langle \hat{\phi}^2 \rangle &= \lim_{x' \rightarrow x, \Delta t=0} \frac{\partial^2}{\partial t^2} G(x, x') \\ &= \frac{c^2}{3r^2} \lim_{\theta' \rightarrow \theta} \left(1 + \frac{\partial^2}{\partial \theta^2} \right) G_R(\theta, \theta'). \end{aligned} \quad (37)$$

(In this and the following subsection, G , G_0 , and G_R refer to relativistic scalar field quantities.) Here $G_R(\theta, \theta') = G(\theta, \theta') - G_0(\theta, \theta')$, where

$$G_0(\theta, \theta') = \frac{\hbar}{16\pi^2 c^3 r^2} \csc^2\left(\frac{\theta - \theta'}{2}\right) \quad (38)$$

is the empty space two-point function, and

$$\begin{aligned} G(\theta, \theta') &= \frac{\hbar}{16\alpha^2 c^3 r^2} \left\{ \csc^2\left[\frac{\pi(\theta - \theta')}{2\alpha}\right] \right. \\ &\quad \left. + \csc^2\left[\frac{\pi(\theta + \theta')}{2\alpha}\right] \right\} \end{aligned} \quad (39)$$

is the two-point function in the presence of the wedge.

We may combine these results to find for the phononic case

$$\begin{aligned} \langle \hat{\rho}^2 \rangle_R &= -\frac{\hbar \rho_0}{1440\pi^2 c_S r^4 \sin^4(\pi\theta/\alpha)} \\ &\quad \times \{(\pi - \alpha)(\pi + \alpha)\sin^2(\pi\theta/\alpha) \\ &\quad \times [(\pi^2 + 11\alpha^2)\sin^2(\pi\theta/\alpha) - 30\pi^2] + 45\pi^4\}. \end{aligned} \quad (40)$$

Again, this quantity is negative everywhere.

D. A cosmic string

As is well known, the space surrounding a cosmic string is a conical space with a deficit angle $\alpha < 2\pi$. Quantum field theory in this conical space has been discussed by many authors, beginning with Helliwell and Konkowski [26], and is similar to the wedge problem discussed above. Equations (37) and (38) hold for the cosmic string as well as the wedge. However, Eq. (39) is replaced by

$$G(\theta, \theta') = \frac{\hbar}{4\alpha^2 c^3 r^2} \csc^2\left[\frac{\pi(\theta - \theta')}{\alpha}\right], \quad (41)$$

which is equivalent to Eqs. (15) and (16) in Ref. [26]. At a distance r from the apex, we find

$$\begin{aligned} \langle \hat{\rho}^2 \rangle_R &= -\frac{\hbar \rho_0}{1440\pi^2 c_S \alpha^4 r^4} (2\pi - \alpha)(2\pi + \alpha) \\ &\quad \times (11\alpha^2 + 4\pi^2), \end{aligned} \quad (42)$$

which is also negative everywhere provided that $\alpha < 2\pi$.

E. Near the focus of a parabolic mirror

The quantization of the electromagnetic field in the presence of a parabolic mirror was discussed by us in Refs. [27,28], where a geometric optics approximation was employed to find the mean squared fields near the focus. This treatment leads to the result that these quantities are singular at the focus, diverging as an inverse power of the distance a to the focus. This result holds both for parabolic cylinders and for parabolas of revolution, and basically arises from the interference term of multiply reflected rays with nearly the same optical path length. The geometry is illustrated in Fig. 1. An incoming ray at an angle of θ reflects at an angle of θ' to reach the point P , which is a distance a from the focus F , as illustrated. The distance from the focus to the mirror itself is $b/2 \gg a$.

The relation between θ and θ' is given by

$$\theta = \frac{a}{b} f(\theta'), \quad (43)$$

where

$$f(\theta') = -\frac{\sin^2 \theta' \sin(\theta' - \gamma)}{(1 - \cos \theta')} = -(1 + \cos \theta') \sin(\theta' - \gamma). \quad (44)$$

Note that θ is defined somewhat differently than in Refs. [27,28], so that $f(\theta)$ now has the opposite sign.

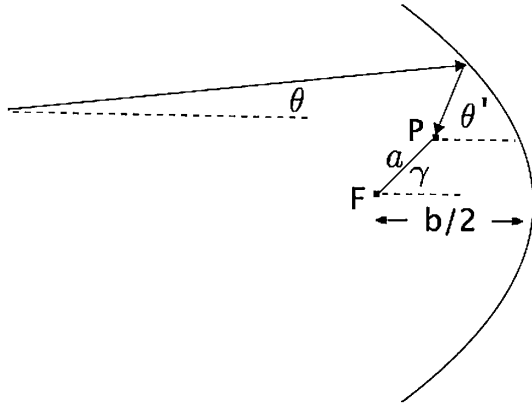


FIG. 1. The geometry of rays reflecting from a parabolic mirror is illustrated. An incoming ray at an angle of θ reflects at an angle of θ' to reach the point P , which is a distance a from the focus F , and at an angle of γ . The distance from the focus to the mirror is $b/2$, as illustrated, where $b \gg a$.

There will be multiply reflected rays whenever different values of θ' are associated with the same value of f . The function $f(\theta')$ is plotted in Fig. 2 for various values of γ . We can see from these plots that, in general, there can be up to four reflected angles θ' for a given incident angle θ . However, if the mirror size θ_0 is restricted to be less than $2\pi/3$, then there will never be more than two values of θ' for a given θ . Throughout this paper, we will assume $\theta_0 < 2\pi/3$, and hence have at most two reflected rays for a given incident ray. The two reflected rays will occur at $\theta' = \alpha$ and $\theta' = \beta$, where

$$f(\alpha) = f(\beta). \quad (45)$$

The difference in the optical paths of these two rays (β path minus α path) is denoted by $\Delta\ell$. The detailed expression for this distance $\Delta\ell$ used in Refs. [27,28] is not quite correct, as was pointed out to us by Vuletic [29]. The expression used in Refs. [27,28], which we will denote by $\Delta\ell_1$, is the difference in distance traveled by the two rays after they cross a line of constant x , perpendicular to the axis of the mirror. This difference is

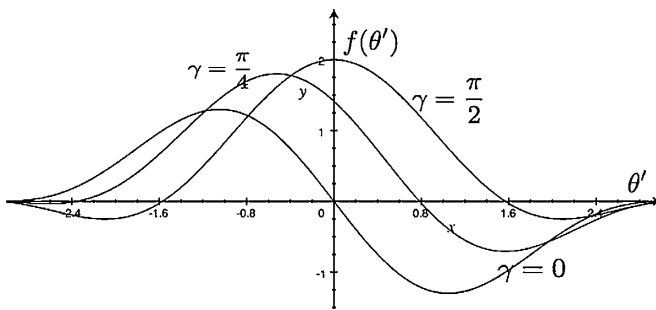


FIG. 2. The function $f(\theta')$ is plotted for various values of γ . This function relates the angle of the incident ray, θ , to the angle of the reflected ray, θ' , through the relation $\theta = (a/b)f(\theta')$.

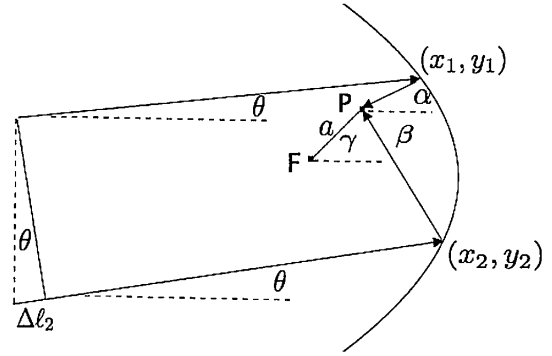


FIG. 3. Two rays reflecting from a parabolic mirror to the point P are illustrated. The first arrives at an angle of $\theta' = \alpha$, and the second at $\theta' = \beta$. The points of intersection with the mirror are (x_1, y_1) and (x_2, y_2) , respectively. The difference in path lengths (lower path minus upper path) is $\Delta\ell = \Delta\ell_1 - \Delta\ell_2$, where $\Delta\ell_2$ is illustrated.

$$\Delta\ell_1 = a[\cos\gamma(\cos\alpha - \cos\beta) + \sin\gamma(\sin\alpha - \sin\beta)]. \quad (46)$$

However, the difference in optical path lengths is the difference in distance traveled after crossing a line perpendicular to the incoming rays, as illustrated in Fig. 3, and is

$$\Delta\ell = \Delta\ell_1 - \Delta\ell_2. \quad (47)$$

The correction term, $\Delta\ell_2$, is

$$\Delta\ell_2 = a[\sin\beta \sin(\beta - \gamma) - \sin\alpha \sin(\alpha - \gamma)]. \quad (48)$$

The corrected expression for $\Delta\ell$ is then

$$\Delta\ell = a[\cos\gamma(\cos\alpha - \cos\beta + \sin^2\alpha - \sin^2\beta) + \sin\gamma(\sin\alpha - \sin\beta + \sin\beta \cos\beta - \sin\alpha \cos\alpha)]. \quad (49)$$

The mean squared electric field near the focus of a parabola of revolution is, in the geometric optic approximation,

$$\langle E^2 \rangle_{\text{pr}} = \frac{3\hbar c}{2\pi^2} \int \frac{d\theta}{(\Delta\ell)^4}. \quad (50)$$

The corresponding expression for a parabolic cylinder is

$$\langle E^2 \rangle_{\text{pc}} = \frac{16}{15\pi} \langle E^2 \rangle_{\text{pr}}. \quad (51)$$

Note that in Eq. (50), the integration is over θ , the angle of the incident ray, not θ' , the reflected angle, as was incorrectly stated in Refs. [27,28].

A detailed discussion of the electromagnetic case will be given elsewhere. Here we are concerned with $\langle \hat{\rho}^2 \rangle_R$ for the parabola of revolution, which is obtained from Eq. (50) by letting $c \rightarrow c_S$ and multiplying by $\rho_0/(2c_S^2)$, leading to the result

$$\langle \hat{\rho}^2 \rangle_R = \frac{3\hbar\rho_0}{4\pi^2 c_S} \int_{\theta_{\min}}^{\theta_{\max}} \frac{d\theta}{(\Delta\ell)^4}. \quad (52)$$

The corresponding expression of a parabolic cylinder is obtained by multiplying by $16/15\pi$. Although the integrand in the above expression is singular at $\Delta\ell = 0$, it may be treated as a distribution and the integral is well defined.

Here we will treat only the case $\gamma = \pi/2$, where the integrations may be done in closed form. In this case, $\beta = -\alpha$, as may be seen from the fact that $f(\theta')$ is now an even function:

$$f(\theta') = (1 + \cos\theta') \cos(\theta'). \quad (53)$$

The minimum value of θ in Eq. (52) is $\theta_{\min} = (a/b)f(\theta_0)$, where θ_0 is the angular size of the mirror. The maximum value in our case is $\theta_{\max} = 2a/b$, corresponding to $\alpha = 0$. We have that

$$\frac{d\theta}{d\alpha} = \frac{a}{b} f'(\alpha) = -\frac{a}{b} \sin\alpha(2\cos\alpha + 1). \quad (54)$$

$$g(\theta_0) = \log\left(\frac{1 + \cos\theta_0}{1 - \cos\theta_0}\right) + \frac{30\cos^5\theta_0 - 120\cos^4\theta_0 + 160\cos^3\theta_0 - 40\cos^2\theta_0 - 94\cos\theta_0 - 224}{15(1 + \cos\theta_0)(1 - \cos\theta_0)^5}. \quad (58)$$

The function $g(\theta_0)$ is negative everywhere, and is plotted in Fig. 4. The singularity as $\theta_0 \rightarrow 0$ represents a breakdown of the geometric optics approximation, as diffraction effects become more important for small θ_0 . For fixed θ_0 , the result is of the form

$$\langle \hat{\rho}^2 \rangle_R = -\frac{\hbar\rho_0 C}{c_S b a^3} < 0, \quad (59)$$

where C is a constant which is small compared to unity.

This, and the analogous expressions for $\langle E^2 \rangle$ and $\langle B^2 \rangle$, which also are proportional to $1/(ba^3)$, are striking in that they can be large when the focus is far from the mirror itself, $b \gg a$. This result is controversial, and seems to be in conflict with a general result by Fewster and Pfenning [30], which implies that quantities such as $\langle E^2 \rangle$ or $\langle \hat{\rho}^2 \rangle_R$ should be proportional to the inverse fourth power of the distance to the mirror, which is to say $\propto b^{-4}$ in this case.

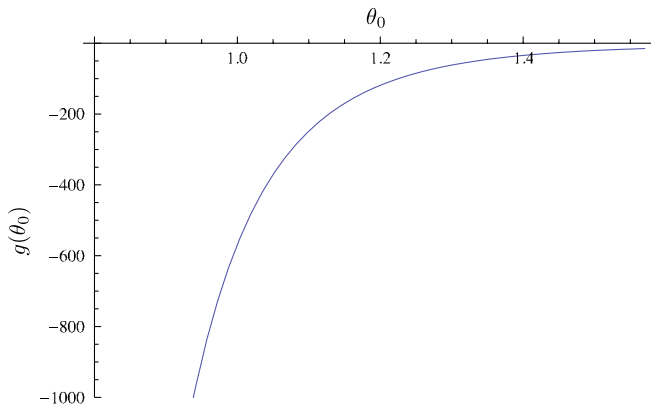


FIG. 4 (color online). The function $g(\theta_0)$, defined in Eq. (58), is plotted.

This relation may be used to express $\langle \hat{\rho}^2 \rangle_R$ as

$$\langle \hat{\rho}^2 \rangle_R = -\frac{3\hbar\rho_0 a}{4\pi^2 c_S b} \int_{\theta_0}^0 d\alpha \frac{\sin\alpha(2\cos\alpha + 1)}{(\Delta\ell)^4}, \quad (55)$$

or as

$$\begin{aligned} \langle \hat{\rho}^2 \rangle_R &= \frac{3\hbar\rho_0}{64\pi^2 c_S a^3 b} \int_0^{\theta_0} d\alpha \frac{2\cos\alpha + 1}{\sin^3\alpha(1 - \cos\alpha)^4} \\ &= \frac{3\hbar\rho_0}{128\pi^2 c_S a^3 b} \int_{-\theta_0}^{\theta_0} d\alpha \frac{2\cos\alpha + 1}{|\sin^3\alpha|(1 - \cos\alpha)^4}. \end{aligned} \quad (56)$$

This integral may be performed explicitly, with the result

$$\langle \hat{\rho}^2 \rangle_R = \frac{3\hbar\rho_0}{4096\pi^2 c_S a^3 b} g(\theta_0), \quad (57)$$

where

On the other hand, there is a simple physical argument to the contrary, which we find compelling: the interference term between multiply reflected rays is slowly oscillating when $\Delta\ell \propto a$ is small, and should give a contribution proportional to an inverse power of a , as in Eq. (59). In any case, the study of the phononic case provides an additional theoretical, and potentially experimental, probe to better understand this issue. Results such as Eq. (59) are potentially observable by light scattering using the method to be discussed in the next section.

VI. OPERATIONAL MEANING OF CHANGES IN $\langle \hat{\rho}^2 \rangle$

In this section, we wish to discuss how changes in $\langle \hat{\rho}^2 \rangle$, or more generally in the density correlation function, $\langle \hat{\rho}(\mathbf{x}, t) \hat{\rho}(\mathbf{x}', t') \rangle$, alter the light scattering cross section. This cross section may be derived from the interaction Hamiltonian used in Ref. [12],

$$H' = \frac{\epsilon_0}{2\rho_0} \int d^3x \hat{\rho}(\mathbf{x}, t) \mathbf{E}^2(\mathbf{x}, t), \quad (60)$$

where \mathbf{E} is the quantized electric field operator. Let the initial state of the photon + phonon system be $|\psi_i\rangle$, containing a photon in mode \mathbf{F}_i and no phonons. The final state is $|\psi_f\rangle$, containing a photon in mode \mathbf{F}_f and one phonon in state $|1_j\rangle$. Here we do not necessarily assume that the photon or phonon modes are plane waves. The transition amplitude in first order perturbation theory is $-i \int dt \langle \psi_f | H' | \psi_i \rangle$, so the transition probability is

$$|\langle \psi_f | H' | \psi_i \rangle|^2 = \frac{\epsilon_0^2}{\rho_0^2} \int dt dt' d^3 x d^3 x' \langle 0 | \hat{\rho}(\mathbf{x}, t) | j \rangle \times \langle j | \hat{\rho}(\mathbf{x}', t') | 0 \rangle M(\mathbf{x}, \mathbf{x}', t, t'), \quad (61)$$

where

$$M(\mathbf{x}, \mathbf{x}', t, t') = \mathbf{F}_f(\mathbf{x}, t) \cdot \mathbf{F}_i^*(\mathbf{x}, t) \mathbf{F}_f^*(\mathbf{x}', t') \cdot \mathbf{F}_i(\mathbf{x}', t'). \quad (62)$$

The total transition probability for the photon involves a sum over all possible phonon modes:

$$T = \sum_j |\langle \psi_f | H' | \psi_i \rangle|^2. \quad (63)$$

However, this is a sum over a complete set of intermediate states, so

$$\langle 0 | \hat{\rho}(\mathbf{x}, t) \hat{\rho}(\mathbf{x}', t') | 0 \rangle = \sum_j \langle 0 | \hat{\rho}(\mathbf{x}, t) | j \rangle \langle j | \hat{\rho}(\mathbf{x}', t') | 0 \rangle. \quad (64)$$

Thus we may write T as an integral involving the density correlation function

$$T = \frac{\epsilon_0^2}{\rho_0^2} \int dt dt' d^3 x d^3 x' \langle 0 | \hat{\rho}(\mathbf{x}, t) \hat{\rho}(\mathbf{x}', t') | 0 \rangle M(\mathbf{x}, \mathbf{x}', t, t'). \quad (65)$$

Here we have set $t' = t$ in the correlation function, because the light scattering occurs on a time scale that is small compared to any changes in the phonon density.

Let T_0 be the scattering probability in the absence of a boundary, which is given by Eq. (65) with the correlation function replaced with the vacuum correlation function given in Eq. (7). Similarly, let T_R be the change in scattering probability due to the boundary, which is given by Eq. (65) using the renormalized correlation function. Then T_R/T_0 is the fractional shift in probability, and hence in scattering cross section, due to the boundary. The integral for T_R has a well-behaved integrand, as the renormalized correlation function G_R is finite as $\mathbf{x}' \rightarrow \mathbf{x}$. However, T_0 has an integrand which diverges as $|\mathbf{x} - \mathbf{x}'|^{-4}$ in this limit, and hence must be defined as a distribution.

Use the identity

$$\frac{1}{|\mathbf{x} - \mathbf{x}'|^4} = \frac{1}{4} \nabla^2 \nabla'^2 \ln[|\mathbf{x} - \mathbf{x}'|^2 / \ell^2]. \quad (66)$$

Here ∇^2 and ∇'^2 are Laplacian operators in \mathbf{x} and \mathbf{x}' , respectively, and ℓ is a constant with units of length, which we take to be of the order of the dimension of the scattering region. We may use this identity in the expression for T_0 and integrate by parts to write

$$T_0 = -\frac{\hbar \epsilon_0^2}{8\pi^2 \rho_0^2 c_S} \int dt dt' d^3 x d^3 x' \ln[|\mathbf{x} - \mathbf{x}'|^2 / \ell^2] \times \nabla^2 \nabla'^2 M(\mathbf{x}, \mathbf{x}', t, t'). \quad (67)$$

The surface terms vanish if we assume that the photon modes are wave packets, so that the overlap function M vanishes outside of the scattering region. The integrand in Eq. (67) now has only an integrable logarithmic singularity.

The corresponding expression for T_R is

$$T_R = \frac{\epsilon_0^2}{\rho_0^2} \int dt dt' d^3 x d^3 x' G_R(\mathbf{x}, \mathbf{x}', 0) M(\mathbf{x}, \mathbf{x}', t, t'). \quad (68)$$

Note that, in general, this depends upon the renormalized phonon two-point function $G_R(\mathbf{x}, \mathbf{x}', 0)$ and not just upon its coincidence limit $\langle \hat{\rho}^2 \rangle_R$. However, if we arrange for the size of the scattering region ℓ to be small compared to the characteristic distance to the boundary, a , then we may write

$$G_R(\mathbf{x}, \mathbf{x}', 0) \approx \langle \hat{\rho}^2 \rangle_R, \quad \ell \ll a. \quad (69)$$

Such a situation is illustrated in Fig. 5. Most of the results in the various cases treated in Sec. V can be written in the form

$$\langle \hat{\rho}^2 \rangle_R = -\frac{\hbar \rho_0 \kappa}{c_S a^4}, \quad (70)$$

where κ is a constant typically smaller than unity. An exception is the case of the parabolic mirror, Eq. (59), which is smaller by a factor of a/b . Let k be the characteristic wave number of the photon mode functions. Then we have

$$\nabla^2 \nabla'^2 M(\mathbf{x}, \mathbf{x}', t, t') \approx k^4 M(\mathbf{x}, \mathbf{x}', t, t'), \quad (71)$$

where we assume that the photon wave packets are peaked around a mean wave number k . Note that we must have

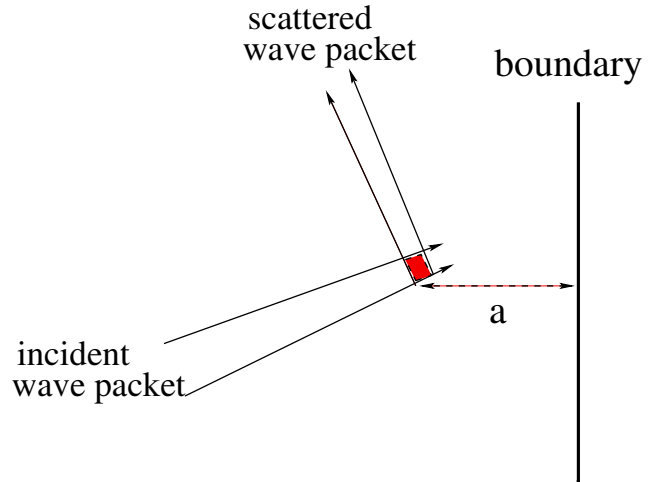


FIG. 5 (color online). The scattering of photon wave packets by a region in the vicinity of a boundary is illustrated. The incident and scattered wave packets overlap in a scattering region (shaded area). Here the characteristic size of this region, ℓ , is assumed to be smaller than the characteristic distance to the boundary, a .

$k > 1/\ell$ so that the wave packets may be localized on a scale of order ℓ .

The logarithm function in Eq. (67) is expected to contribute a factor of order unity, so we obtain the estimate

$$\left| \frac{T_R}{T_0} \right| \approx \frac{8\pi^2 \kappa}{(ka)^4} \quad (72)$$

for the cases for which Eq. (70) holds, and the estimate

$$\left| \frac{T_R}{T_0} \right| \approx \frac{8\pi^2 \kappa}{k^4 b a^3} \quad (73)$$

for the parabolic mirror. Clearly the limit which we have discussed, where $ka \gg 1$, leads to $|T_R T_0| \ll 1$, so the modification of the scattering cross section is a small effect. Consider the case of a single mirror, where from Eq. (31), we have $\kappa = 1/(32\pi^2)$. If we were to take $ka \approx 10$, then we would estimate $|T_R/T_0| \approx 3 \times 10^{-5}$. Given that the scattering effect predicted in Ref. [12] for a boundaryless fluid has not yet been observed, observation of the effect of boundaries seems to be beyond the limits of present technology. However, this pessimistic conclusion is partly based upon the restriction that $ka \gg 1$. If this restriction is removed, and one uses light for which $ka \approx 1$, a larger effect is likely. This cannot be accurately computed from the analysis in this section, but one might expect the effect of the boundary to become closer to that in the boundaryless fluid.

VII. SUMMARY AND DISCUSSION

In this paper, we have treated the effects of squeezed phonon states and of boundaries on the local quantum density fluctuations of a fluid, assuming a linear phonon dispersion relation. The purpose of this investigation is twofold. The modified density fluctuations are of interest in their own right and are, in principle, observable by light or neutron scattering. Second, the phononic system studied here is a potentially useful analog model for better understanding quantum fluctuations in relativistic quantum field theory with boundaries. After reviewing the density fluctuations in a boundaryless system in the phonon vacuum state, we treated the effects of a squeezed vacuum state of phonons. Here we found that such a state will have both local increases and local decreases in the mean squared density. However, the time or spatial averaged effect is an increase. This is in complete analogy to the case in relativistic quantum field theory, with the decrease in mean squared density corresponding to regions of negative energy density.

We next turned our attention to the effects of perfectly reflecting boundaries and studied the cases of one and two parallel plates, a torus, a wedge, a cosmic string, and a

parabolic mirror. In all of the cases examined, we found a decrease in mean squared density, $\langle \hat{\rho}^2 \rangle_R < 0$. This amounts to a suppression of the usual zero-point fluctuations, and is analogous to the suppression of vacuum fluctuations which can lead to negative energy density in quantum field theory. In general, $\langle \hat{\rho}^2 \rangle_R$ due to boundaries is inversely proportional to the speed of sound, c_S . This is in contrast to total energies or forces, such as Eq. (21), which are proportional to c_S , and to the mean squared electric or magnetic fields near a perfect reflector, Eqs. (22) and (23), which are proportional to the speed of light.

The case of the parabolic mirror is of particular interest. Here we were able to correct certain aspects of our previous treatment [27,28] for electromagnetic fields. We find that near the focus, $\langle \hat{\rho}^2 \rangle_R$ grows as the inverse cube of the distance to the focus. For the phononic case, this growth necessarily stops as the scale of interatomic spacing is reached. However, the analysis performed here for phonons also applies to the case of the quantized electromagnetic field, where one expects the same rate of growth in the mean squared electric and magnetic fields.

In this paper, we have considered only the case of a linear dispersion relation. For the types of effect we consider, this should be a good approximation so long as the distance to the boundary is large compared to the interatomic spacing. However, the effects of nonlinearity become important if one wishes to consider event horizons rather than physical boundaries. There has been considerable interest in recent years in analog models of black hole and other horizons [8,31–33].

Finally in Sec. VI, we derived an expression for the fractional change in scattering probability due to the presence of the boundary. In the limit treated here, where the size of the scattering region is small compared to the distance to the boundary, $\ell \ll a$, we obtained a small fractional change which scales as $(\ell/a)^4$ in most cases. If it is possible to relax this restriction and treat cases where ℓ/a becomes of order unity, then we can expect a larger change in the scattering cross section. However, this will require further analysis using the complete expression for T_R , given in Eq. (68). This will be the topic of future research.

ACKNOWLEDGMENTS

This work was supported in part by the National Science Foundation under Grant No. PHY-0855360 and by Conselho Nacional de Desenvolvimento Científico e Tecnológico do Brasil (CNPq). L. H. F. would like to thank the Institute of Physics at Academia Sinica in Taipei and National Dong Hwa University in Hualien, Taiwan for hospitality while this manuscript was completed.

- [1] I. E. Dzyaloshinskii, E. M. Lifshitz, and L. P. Pitaevski, *Adv. Phys.* **10**, 165 (1961).
- [2] A. Larraza, *Phys. Lett. A* **248**, 151 (1998).
- [3] O. Bschorr, *J. Acoust. Soc. Am.* **106**, 3730 (1999).
- [4] E. Schäffer and U. Steiner, *Eur. Phys. J. E* **8**, 347 (2002).
- [5] D. C. Roberts and Y. Pomeau, *Phys. Rev. Lett.* **95**, 145303 (2005).
- [6] A. Recati, J. N. Fuchs, C. S. Peça, and W. Zwerger, *Phys. Rev. A* **72**, 023616 (2005).
- [7] S. K. Lamoreaux, arXiv:0808.4000.
- [8] W. G. Unruh, *Phys. Rev. Lett.* **46**, 1351 (1981); *Phys. Rev. D* **51**, 2827 (1995).
- [9] L. H. Ford and N. F. Svaiter, *J. Phys. Conf. Ser.* **161**, 012034 (2009).
- [10] See, for example, E. M. Lifshitz and L. P. Pitaevski, *Statistical Physics, Part 2* (Pergamon, Oxford, 1969), 2nd ed., Eq. (24.10).
- [11] P. O. Fedichev and U. R. Fischer, *Phys. Rev. A* **69**, 033602 (2004).
- [12] L. H. Ford and N. F. Svaiter, *Phys. Rev. Lett.* **102**, 030602 (2009).
- [13] Note that the thermal Brillouin scattering cross section cited in Eq. (25) of Ref. [12] is actually the high temperature limit of the total Brillouin cross section and hence twice the Stokes line cross section. This compensates for the fact that $1/2$ of the zero-point part is canceled by the thermal correction. Thus the ratio R in Eq. (27) of Ref. [12] is still correct.
- [14] A. L. Fetter, *J. Low Temp. Phys.* **6**, 487 (1972).
- [15] R. P. Feynman and M. Cohen, *Phys. Rev.* **102**, 1189 (1956).
- [16] C. M. Caves, *Phys. Rev. D* **23**, 1693 (1981).
- [17] J. C. Garrison and R. Y. Chiao, *Quantum Optics* (Oxford University Press, Oxford, 2008).
- [18] Chung-I Kuo and L. H. Ford, *Phys. Rev. D* **47**, 4510 (1993).
- [19] A. Borde, L. H. Ford, and T. A. Roman, *Phys. Rev. D* **65**, 084002 (2002).
- [20] R. L. Jaffe, *AIP Conf. Proc.* **687**, 3 (2003).
- [21] K. A. Milton, I. Cavero-Pelaez, and J. Wagner, *J. Phys. A* **39**, 6543 (2006).
- [22] V. Sopova and L. H. Ford, *Phys. Rev. D* **72**, 033001 (2005).
- [23] L. H. Ford and N. F. Svaiter, *Phys. Rev. D* **58**, 065007 (1998).
- [24] R. B. Rodrigues and N. F. Svaiter, *Physica A (Amsterdam)* **328**, 466 (2003).
- [25] D. Deutsch and P. Candelas, *Phys. Rev. D* **20**, 3063 (1979).
- [26] T. M. Helliwell and D. A. Konkowski, *Phys. Rev. D* **34**, 1918 (1986).
- [27] L. H. Ford and N. F. Svaiter, *Phys. Rev. A* **62**, 062105 (2000).
- [28] L. H. Ford and N. F. Svaiter, *Phys. Rev. A* **66**, 062106 (2002).
- [29] V. Vuletic (private communication).
- [30] C. J. Fewster and M. J. Pfenning, *J. Math. Phys. (N.Y.)* **47**, 082303 (2006).
- [31] T. Jacobson, *Phys. Rev. D* **44**, 1731 (1991).
- [32] C. Barcelo, S. Liberati, and M. Visser, *Living Rev. Relativity* **8**, 12 (2005).
- [33] P. O. Fedichev and U. R. Fischer, *Phys. Rev. Lett.* **91**, 240407 (2003).